

The Impact of Inhomogeneous Reionization on Cosmic Microwave Background Anisotropy

Lloyd Knox¹, Román Scoccimarro¹, and Scott Dodelson²

¹ Canadian Institute for Theoretical Astrophysics, Toronto, ON M5S 3H8, CANADA

² NASA/Fermilab Astrophysics Center

Fermi National Accelerator Laboratory, Batavia, IL 60510, USA

(February 7, 2020)

Hydrogen atoms in the Universe that initially formed at redshift $z \simeq 1100$ were reionized at $5 \lesssim z \lesssim 60$. It is likely that this transition proceeded through a mixed phase of partial ionization. We develop an analytic approach to calculating the effect on the cosmic microwave background (CMB) of Thomson scattering off this inhomogeneous distribution of free electrons. We study two models of the reionization process, one of which associates ionized patches with overdense regions of the smoothed density field. We find the generated anisotropy to have a power spectrum which peaks at angular scales corresponding to the extent of the ionized regions, and has a width that reflects the correlations between them. There is considerable uncertainty in the amplitude, which depends on how efficiently collapsed objects can reionize the surrounding medium. We calculate the effect of neglecting inhomogeneous reionization in the determination of cosmological parameters from high resolution CMB maps and find that it may be a significant source of systematic error.

Introduction. Observations of cosmic microwave background (CMB) anisotropy are providing strong constraints on theories of cosmological structure formation. Planned CMB observations can potentially provide constraints on the parameters of these theories at the percent level [1,2]. One of the reasons the CMB is such a wonderful probe of cosmological parameters is that predictions for a given theory can be made with great precision [3]. This is because linear perturbation theory is an excellent approximation over the relevant length scales at $z \simeq 1100$ when the CMB was last tightly coupled to matter.

However, new anisotropies can be generated at late times by the non-linear process of reionization as the CMB photons are brought back into contact with matter via Thomson scattering. We know this reionization took place before redshift $z \simeq 5$ because spectra of distant quasars do not show a continuum of absorption by neutral hydrogen. It is unlikely that reionization occurred at $z \gtrsim 60$ for in that case the level of anisotropies on degree scales would be significantly lower than on ten degree scales. Dozens of recent experiments have shown that just the opposite is true: there is more power on degree scales than on larger scales [4].

Reionization affects the CMB anisotropies in several ways. First, the fluctuation power on small angular scales is suppressed by a factor $e^{-2\tau}$ where τ is the optical depth back to last scattering. Second, as Sunyaev and Kaiser [5] pointed out, secondary anisotropies are generated on large scales due to the Doppler effect when photons scatter off moving free electrons. They also noted that the effect is strongly suppressed on small scales because photons get nearly opposite Doppler shifts on different sides of a density peak, a consequence of potential flows generated by gravitational instability. Both of these effects—the damping and the Sunyaev-Kaiser

(SK) effect—are linear and therefore included in standard Boltzmann codes [3].

Here we focus on the effects of inhomogeneities in the ionization field [6–8]. We show that inhomogeneous reionization (IHR) restores the SK effect at small scales due to modulation of the velocity field with the spatial variation of the ionization fraction. Since the typical patch size is much smaller than the scale of variation of the velocity field, the Doppler effect contributions come only from regions where the flow is coherent.* The resulting anisotropy pattern depends sensitively on the model of reionization. Thus, the signature of IHR in the CMB provides an indirect window on a poorly probed but interesting era in which the first stars and galaxies formed. On the other hand, if these anisotropies are large enough, they can create systematic errors in the determination of cosmological parameters. So, after calculating the anisotropies, we compute the magnitude of these systematic errors, i.e. how much a given cosmological parameter might be *misestimated* if IHR is ignored.

Anisotropy Spectrum: Formal Solution. The perturbation to the photon temperature distribution function, $\Delta \equiv \delta T/T$, is governed by the Boltzmann equation, which at the late times of interest is

$$\partial \Delta(\mathbf{x}, \eta, \hat{\gamma}) / \partial \eta = n_e \sigma_T a \hat{\gamma} \cdot \mathbf{v}(\mathbf{x}, \eta) \quad (1)$$

where $a = (1+z)^{-1}$ is the scale factor of the universe normalized to unity today, $\eta \equiv \int dt/a$ is the conformal time, n_e is the free electron density, σ_T is the Thomson

* This is analogous to the modulation caused by the density field, which appears in the homogeneous case through second-order perturbation theory [9].

cross-section, $\hat{\gamma}$ is the direction of the photon momentum, and \mathbf{v} is the electron velocity. Henceforth we work in units where the conformal time today is unity, $\eta_0 = 1$; and assume a flat, matter dominated universe, $a = \eta^2$. The solution to Eq. 1 for the photon perturbations here and now (at $\mathbf{x} = \mathbf{x}_0$ and $\eta = 1$; $\Delta_0(\hat{\gamma}) \equiv \Delta(\mathbf{x}_0, \eta_0, \hat{\gamma})$) is

$$\Delta_0(\hat{\gamma}) = 4.06 \times 10^{-5} \Omega_b h \int_{\eta_i}^1 \frac{d\eta}{\eta^3} \chi(\mathbf{x}, \eta) \hat{\gamma} \cdot \mathbf{v}(\mathbf{x}), \quad (2)$$

where, $\mathbf{v}(\mathbf{x}, \eta) \equiv -2\eta \mathbf{v}(\mathbf{x})$ (Mpc/h), $n_e = \bar{n}_e \chi(\mathbf{x}, \eta) a^{-3}$, and $\bar{n}_e \sigma_T \eta_0 = 0.122 \Omega_b h$, with \bar{n}_e the present mean electron density, Ω_b the density of baryons in units of the critical density and h the Hubble constant in units of 100 km s⁻¹ Mpc⁻¹. Both χ and \mathbf{v} are evaluated at $\mathbf{x} = \mathbf{x}_0 - \hat{\gamma}(1 - \eta)$, the position at time η of a photon with direction vector $\hat{\gamma}$ incident on us today. Note that the integral includes all contributions starting from η_i , a time far after standard recombination at $\eta \simeq 0.03$, but before reionization occurs.

Our predictions are necessarily statistical in nature. We focus on the two-point correlation function:

$$C(\theta) \equiv \langle \Delta_0(\hat{\gamma}) \Delta_0(\hat{\gamma}') \rangle ; \quad \cos \theta \equiv \hat{\gamma} \cdot \hat{\gamma}', \quad (3)$$

where the angular brackets indicate an average over all locations \mathbf{x}_0 . Using Eq. 2 we obtain the correlation function due to reionization:

$$C(\theta) = 10^{-12} \left(\frac{\Omega_b h}{0.025} \right)^2 \int_{\eta_i}^1 \frac{d\eta}{\eta^3} \int_{\eta_i}^1 \frac{d\eta'}{\eta'^3} \mathcal{C}(\eta, \eta', \theta). \quad (4)$$

It is therefore determined by an integral over adjacent lines of sight of the four-point correlation function

$$\mathcal{C}(\eta, \eta', \theta) \equiv \hat{\gamma}_i \hat{\gamma}'_j \langle \chi \chi' v_i v'_j \rangle, \quad (5)$$

where, for example, $\chi' \equiv \chi(\mathbf{x}', \eta')$. Different models of reionization will lead to different four-point functions. We now explore several possibilities.

Homogeneous Reionization. The simplest possibility is that reionization takes places homogeneously. While not particularly plausible, it is a useful limiting case for demonstrating the SK cancellation. In homogeneous reionization (HR), $\chi \equiv \bar{\chi}(\eta)$, where $\bar{\chi}$ is fraction of the Universe that is ionized. Thus we have:

$$\mathcal{C}^{\text{HR}}(\eta, \eta', \theta) = \bar{\chi} \bar{\chi}' C_v(\eta, \eta', \theta) \quad (6)$$

and we take $\bar{\chi}$ to be zero at times earlier than $z_i + \delta z_i$, unity at times later than z_i and to increase linearly with redshift during the transition. The velocity correlation function can be written as

$$C_v(\eta, \eta', \theta) = \Psi_{\perp} \cos \theta + (\Psi_{\parallel} - \Psi_{\perp}) \frac{(\mathbf{r} \cdot \hat{\gamma}) (\mathbf{r} \cdot \hat{\gamma}')}{r^2}, \quad (7)$$

where $\mathbf{r} \equiv \mathbf{x} - \mathbf{x}'$. The correlation functions of the velocity components parallel and perpendicular to \mathbf{r} are

$$\Psi_{\parallel}(r) = \int \frac{P(k)}{k^2} \left[j_0(kr) - 2 \frac{j_1(kr)}{kr} \right] d^3 k, \quad (8)$$

$$\Psi_{\perp}(r) = \int \frac{P(k)}{k^2} \frac{j_1(kr)}{kr} d^3 k, \quad (9)$$

where $P(k)$ is the matter power spectrum, throughout assumed to be that of the standard cold dark matter theory of structure formation, as given in [10]. Fig. 1 shows $C_v(\eta, \eta', 0)$ as a function of η for fixed $\eta' = 0.188$. C_v is strongly peaked at equal times, since the two lines of sight share the same velocity. On the other hand, at large $|\eta - \eta'|$, C_v becomes negative due to infall from opposite sides into an overdense region. Since η is only varying by a small amount between the start and end of reionization, the integration of this oscillatory function with slowly-varying functions of time in Eq. 4 leads to a cancellation of Doppler effects, as described by Kaiser [5] in Fourier space.

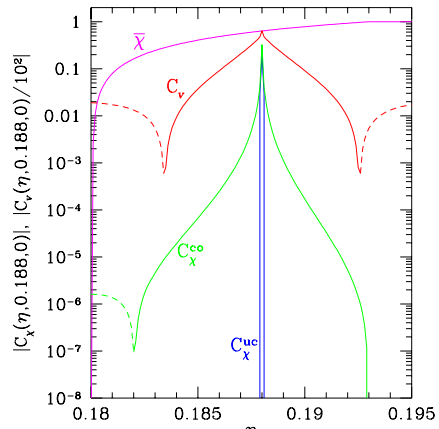


FIG. 1. The mean ionization fraction $\bar{\chi}$ for HR ($z_i = 26$, $\delta z_i = 4$), the velocity two-point function $C_v(\eta, 0.188, 0)$ for the SCDM (standard cold dark matter) model with $\sigma_8 = 1.2$ where σ_8 is the rms of mass fluctuations in spheres of radius $8h^{-1}$ Mpc today, and the ionization fraction two-point function for uncorrelated C_x^{uc} and correlated bubbles C_x^{co} . Dashed lines denote negative values.

Uncorrelated Inhomogeneous Reionization. The SK cancellation can be avoided if the velocity two-point function C_v is modulated by the spatial dependence of the ionization fraction. Indeed, such modulation is expected on scales of order the size of an ionized region. To demonstrate this effect, we adopt a simple toy model of the reionization process. In this model sources turn on randomly and instantaneously ionize a sphere with comoving radius R and volume V_R . We further assume that these spheres remain ionized (which is most accurate at lower redshifts when the recombination rate is lower). This picture implies that correlations exist between χ and χ' only if the distance between them satisfies $r \leq 2R$. More quantitatively, the model implies

$$C^{\text{uc}}(\eta, \eta', \theta) = C_v(\eta, \eta', \theta) C_x^{\text{uc}}(\eta, \eta', \theta), \quad (10)$$

$$C_\chi^{\text{uc}} = (1 - \bar{\chi})(1 - \bar{\chi}') \left[(1 - \bar{\chi}_{\min})^{-V_o(r)/V_R} - 1 \right], \quad (11)$$

where $\chi_{\min} \equiv \chi(\min(\eta, \eta'))$. The volume of overlap $V_o(r)$ is the volume of the region in which a single source could ionize both locations \mathbf{x} and \mathbf{x}' . It is (for $r \leq 2R$)

$$V_o(r) = V_R [1 - (3/4)(r/R) + (1/16)(r/R)^3], \quad (12)$$

and zero otherwise. The resulting two-point function, C_χ^{uc} , is sharply peaked at small $r \approx |\eta - \eta'|$ (see Fig. 1, where $R = 1$ Mpc), therefore in Eq. 10, $C_v(\theta) \propto C_v(\eta, \eta, \theta)$. Thus, the SK cancellation of homogeneous reionization is avoided; IHR modulates the velocity field, accessing only the region where the velocity field is highly coherent. Note though that the modulation is not particularly effective since the ionization radius R is typically very small, and thus only a tiny region of η contributes. Therefore, as Gruzinov and Hu (GH) [7] have pointed out, a model of this type necessarily produces anisotropies which have amplitude proportional to R .

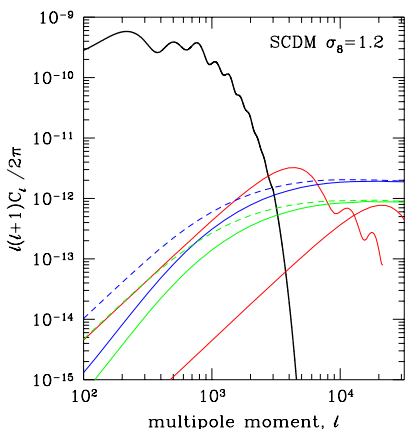


FIG. 2. The angular power spectrum, C_l , defined by $C(\theta) \equiv \sum_l (2l + 1)C_l/(4\pi)P_l(\cos\theta)$. The thick solid line on top is the linear spectrum. The rest are different approximations to the IHR anisotropies, all assuming $\Omega_b = 0.1$ and $h = 0.5$. The curves peaked at $l = 4000$ and $l = 20000$ are from the uncorrelated $R = 5$ Mpc and $R = 1$ Mpc models respectively. The dashed curves show the model of Eq. 14 for $z_i = 26$ (bottom) and $z_i = 31$ (top). Solid lines include velocity-ionization field cross-correlations.

Figure 2 shows the anisotropy spectrum arising from the two-point function of Eq. 10, assuming $z_i = 26$ and $\delta z_i = 4$. Not shown, to avoid clutter, are the GH results for the same parameter choices. These would each have peaks 30% lower in l and two times larger in amplitude due to a slower fall off of C_χ^{uc} with r and one less factor of $(1 - \bar{\chi})$ in their version of Eq. 11. Despite these differences, they correctly identified the qualitative features of this type of inhomogeneous reionization: (i) amplitude proportional to R ; (ii) white noise ($C_l^{\text{IHR}} \propto \text{constant}$) on large scales due to lack of correlations at $r \gg R$; and (iii) peak at $l \sim (1 - \eta_r)/R$ where reionization takes place

at η_r . We now show that the first two of these features break down when more realistic models are considered.

Correlated Inhomogeneous Reionization. Because the ionizing sources in the model of Eq. 11 and that devised by GH are independent of each other, correlations in the ionization field only exist on scales comparable to, or smaller than, the ionization radius R . However, overdense regions, such as galaxies and clusters of galaxies, are observed to be highly correlated with each other. If overdense regions are the sources of the ionizing radiation (which they are very likely to be) then their clustering will lead to long-range correlations in the ionization field and therefore affect $C^{\text{IHR}}(\theta)$.

The physical process we imagine is that the mass in any region where the linear theory density contrast smoothed on a comoving scale R_c , δ_{R_c} , exceeds a critical threshold ($\delta_c = 1.69$), collapses, forms stars or quasars which then ionize a region with size $R = E^{1/3}R_c$. The efficiency, E , is the ratio of the volume of the ionized regions to collapsed regions. From this scenario we expect [10,14]

$$\bar{\chi} = 2E \int_{\delta_c}^{\infty} d\delta P_{R_c}(\delta) = E \text{erfc}\left(\frac{\delta_c}{\sqrt{2}\sigma_{R_c}(\eta)}\right), \quad (13)$$

$$\begin{aligned} C_\chi^{\text{co}} = \langle \chi \chi' \rangle &= \alpha \alpha' \int_{\delta_c}^{\infty} d\delta \int_{\delta_c}^{\infty} d\delta' P_{R_c}(\delta, \delta') \\ &\approx \frac{\alpha \alpha'}{2\pi} \frac{\Xi_{R_c}(r)}{\sigma_{R_c}(\eta) \sigma_{R_c}(\eta')} \exp\left[-\frac{\nu^2(\eta) + \nu^2(\eta')}{2}\right], \end{aligned} \quad (14)$$

where $\text{erfc}(x)$ denotes the complementary error function, $\alpha \equiv 2E(1 - \bar{\chi})$, $P_{R_c}(\delta)$ and $P_{R_c}(\delta, \delta')$ are the one and two-point distributions of the smoothed field δ_{R_c} , respectively; the smoothed correlation function is given by $\langle \delta \delta' \rangle \equiv \Xi_{R_c}(r)$, $\sigma_{R_c} \equiv \Xi_{R_c}(0)$, and $\nu(\eta) \equiv \delta_c/\sigma_{R_c}(\eta)$.

Despite a number of studies of the details of reionization [11–13], we are still far from a satisfactory understanding. Therefore, we take two simple models for the efficiency of reionization, which can vary by many orders of magnitude (see e.g. table 2 in [12]). The requirement that objects more massive than $M_c(z) \simeq 10^8 M_\odot [10/(1+z)]^{3/2}$ are necessary for reionization [13] leads to a smoothing scale of $R_c = 0.22\eta$ Mpc, and therefore an efficiency $E = 7 \times 10^5 \eta^6$, and $z_i = 26$. For comparison, we also take an effective efficiency $E = 114$ as the “middle of the road” model in [12], which gives $z_i = 31$ for the same mass-scale. Note that current scenarios for reionization generally lead to $E \gg 1$, i.e. the sources tend to ionize a region much larger than their typical volume (see however [8] for a different view).

Fig. 1 shows the results of Eq. 14 for the $z_i = 26$ model. The clustering of overdense regions naturally leads to a much wider C_χ^{co} , which falls off only as a power-law, thus more efficiently modulating C_v . For this reason, the correlated models in Fig. 2 (dashed lines) show a much wider distribution of power, and the white noise regime is only reached at scales considerably larger than the patch size. Over the range of ℓ plotted, the power spectrum of

the uncorrelated models with the same values of R as in the peaks model would be orders of magnitude smaller. The solid lines show the effect of including the cross-correlations of the ionization fraction with the velocity field [15], which leads to a modification of the white noise behavior at large scales. Note that the flatness of the power spectra in Fig. 2 above $\ell \simeq 3000$ reflects the near scale-invariance of the matter power spectrum over the relevant length scales.

Impact on Parameter Determination. The anisotropies produced during inhomogeneous reionization can potentially spoil the exquisite parameter determination anticipated from future CMB observations. Suppose a multi-dimensional fit is performed on the data to extract a set of parameters $\{p_i\}$. If the fit assumes $C_l(\{p_i\})$ that ignores the contribution from C_l^{IHR} , then each parameter will be incorrectly estimated by an amount

$$\Delta p_i = F_{ij}^{-1} \sum_l w_l \frac{\partial C_l}{\partial p_j} C_l^{\text{IHR}} \quad (15)$$

where the weights w_l are the inverse of the squares of the errors expected on C_l 's (the errors are the sum of the errors due to sample variance and those due to noise [1,2]); F_{ij} is the Fisher matrix $\sum_l w_l (\partial C_l / \partial p_i)(\partial C_l / \partial p_j)$. Table 1 shows, for Planck[†], the ratio of this systematic offset to the statistical uncertainty.[‡] Since IHR affects very small scales, MAP[§] is not sensitive to this offset.

Sources of Uncertainty. Even within the context of our peaks model, Eq. 14 is not exact. Since the ionized region is larger than the region that collapsed (i.e., $E > 1$) a more rigorous approach would be to calculate the probability of two points both being within a distance R of one or more peaks. Instead, we have calculated the probability that two points are both *within* a peak and then scaled the resulting two-point function by EE' . We expect this to be a good approximation for $r > R$, which covers the angular range of relevance for the curves in Fig. 2. Because we have not taken the more rigorous approach, we must include suppression factors to correct for overcounting overlapping regions. These are the factors of $(1 - \bar{\chi})$, motivated by their appearance in our fully tractable uncorrelated model. Removing them boosts the power spectrum by a factor of about 4.

Uncertainty in E has a much milder effect on uncertainty in C_l^{IHR} than one might expect from a quick glance

at Eq. 14. The reason is that increasing E causes reionization to occur earlier and therefore decreases the exponential factor in Eq. 14. We find that decreasing E by a factor of 10 decreases C_l^{IHR} by a factor of two.

Our peaks model, and the calculations which lead to the estimates of its parameters, are still highly idealized. Details specific to each collapsing region will lead to a spread of efficiencies and patch sizes. The larger sizes and efficiencies will provide the dominant contribution to C_l^{IHR} . To the extent that local details are important, the transition globally may be broadened, increasing C_l^{IHR} . Although these uncertainties influence the details of our results, we believe that significant power at scales larger than the patch size is a natural consequence of cosmic structure formation via gravitational instability.

ACKNOWLEDGMENTS

We thank J.R. Bond, D. Pogosyan and A. Stebbins for useful discussions, and JRB for the C_l derivatives. SD is supported by the DOE and by NASA Grant NAG 5-7092.

- [1] L. Knox, *Phys. Rev.* **D52**, 4307 (1995); G. Jungman, M. Kamionkowski, A. Kosowsky & D.N. Spergel, *Phys. Rev. Lett.* **76**, 1007 (1996); *ibid*, *Phys. Rev.* **D54**, 1332 (1996); M. Zaldarriaga, D. Spergel & U. Seljak, *Astrophys. J.* **488**, 1 (1997).
- [2] J.R. Bond, G. Efstathiou & M. Tegmark, *MNRAS* **291**, L33 (1997).
- [3] See e.g. P.J.E. Peebles & J.T. Yu, *Astrophys. J.* **162**, 815 (1970); J.R. Bond & G. Efstathiou, *Astrophys. J.* **285**, L45 (1984); U. Seljak and M. Zaldarriaga, *Astrophys. J.* **469**, 437 (1996).
- [4] See e.g. D. Scott and M. White, in the Proceedings of the CWRU CMB Workshop “2 years after COBE” eds. L. Krauss & P. Kernan (1994); S. Hancock, G. Rocha, A. N. Lasenby & C.M. Gutierrez, *MNRAS* **294**, L1 (1998).
- [5] R.A. Sunyaev in *Large-Scale Structure of the Universe*, eds. M.S. Longair & J. Einasto (Dordrecht: Reidel), p. 393 (1978); N. Kaiser, *Astrophys. J.* **282**, 374 (1984).
- [6] N. Aghanim, F.X. Desert, J.L. Puget, & R. Gispert, *Astron. Astrophys.* **311**, 1 (1996).
- [7] A. Gruzinov & W. Hu, *astro-ph/9803188* (1998).
- [8] P.J.E. Peebles & R. Juszkiewicz, *astro-ph/9804260* (1998).
- [9] J.P. Ostriker & E. Vishniac, *Astrophys. J.* **306**, L51 (1986); E. Vishniac, *Astrophys. J.* **322**, 597 (1987).
- [10] J.M. Bardeen, J.R. Bond, N. Kaiser, & A.S. Szalay, *Astrophys. J.* **304**, 15 (1986).
- [11] B.J. Carr, J.R. Bond, & W.D. Arnett, *Astrophys. J.* **277**, 445 (1984); H.M.P. Couchman & M.J. Rees, *MNRAS* **221**, 53 (1986); M. Fukugita & M. Kawasaki, *MNRAS* **269**, 563 (1994); P.R. Shapiro, M.L. Giroux, & A.

[†] <http://astro.estec.esa.nl/SA-general/Projects/Planck>

[‡]This does not include polarization information; however, since polarization is sourced by the quadrupole moment, not the electron velocity, the polarization IHR power spectrum will be down by roughly a factor of $(10^{-5}/10^{-3})^2$ from the IHR temperature power spectrum.

[§]<http://map.gsfc.nasa.gov>

Babul, *Astrophys. J.* **427**, 25 (1994); J.P. Ostriker & Y.N. Gnedin, *Astrophys. J.* **486**, 581 (1997).

[12] M. Tegmark, J. Silk, & A. Blanchard, *Astrophys. J.* **434**, 395 (1995).

[13] Z. Haiman & A. Loeb, *Astrophys. J.* **483**, 21 (1997); *ibid*, astro-ph/9710208 (1997).

[14] N. Kaiser, *Astrophys. J.* **284**, L9 (1984).

[15] L. Knox, R. Scoccimarro, & S. Dodelson, *in preparation* (1998).

model	n_s	r_{ts}	τ	$\Omega_b h^2$	$\Omega_{\text{vac}} h^2$	$\Omega_m h^2$	$\Omega_\nu h^2$
$z_i = 31$	0.75	0.65	0.01	2.25	0.20	-1.02	0.94
$z_i = 26$	0.34	0.29	0.006	1.01	0.09	-0.46	0.42

TABLE I. Ratio of systematic offset to statistical uncertainty expected for the Planck experiment from the two “peaks” models in Fig. 2. Variables are, from left to right, the primordial power spectrum index, the ratio of tensor to scalar contributions to C_2 , the optical depth and the contribution to h^2 from (b)aryons, (curv)ature, cold dark (m)atter and massive neutrinos. The power spectrum derivatives were evaluated at the parameter values of the SCDM model in [2].